Advances in Computational Design, *Vol. 10, No. 3 (2025) 211-232*
https://doi.org/10.12989/acd.2025.10.3.211

Exact thermo-mechanical response of functionally graded cylinders under combined loading

Sanjay Kumar Singh[1], Lakshman Sondhi[2], Rakesh Kumar Sahu[3], Royal Madan*[4] and Anil Prakash Singh[5]

[1]*Department of Mechanical Engineering, Chhatrapati Shivaji Institute of Technology, Durg, India*
[2]*Department of Mechanical Engineering, Shri Shankaracharya Technical Campus, Bhilai, India*
[3]*Department of Mechanical Engineering, Visvesvaraya National Institute of Technology, Nagpur, India*
[4]*Department of Mechanical Engineering, Graphic Era (Deemed to be University), Dehradun 248002, Uttarakhand, India*
[5]*Maharana Pratap Polytechnic, Gorakhpur, 273015, India*

(Received April 3, 2025, Revised June 19, 2025, Accepted July 10, 2025)

Abstract. Functionally graded materials (FGMs) are advanced materials with varying material properties directionally. The material properties, such as elastic modulus, density, thermal conductivity, and thermal expansion coefficient, improve by combining different materials. The structure thus offers a better strength-to-weight ratio, thermal resistance, and durability in critical harsh environments. In the present study, material properties follow a power law for material gradation along the thickness of the cylinder. Navier's approach is followed to solve the second-order governing differential equations with the assumption of a plane stress condition to eliminate the complexity of differential equations, and MATLAB was used to solve stress and deformation variation analytically and for visualization. This research aims to provide an exact solution to stress and deformation for different real-life complex loading conditions with material non-homogeneity. It is essential to analyze various loading conditions to maximize the structure's lifecycle, minimizing the stresses induced. This analysis provides valuable insight to enhance the performance, reliability, and integrity of structures in the fields of aerospace, defense, mechanical, and civil. This research also provides a prominent connection for practical application to designing/analysis.

Keywords: FGM; hollow cylinder; material grading laws; Navier's method; thermo-mechanical analysis

1. Introduction

Composite materials are materials that provide enhanced properties compared to their constituents (fiber and matrix). In composites, it is required that the properties will be constant throughout, which means the reinforcement is distributed uniformly over the matrix (Al-Furjan *et al*. 2022, Amirjan and Bozorg 2019). On the other hand, functionally graded materials (FGMs) are advanced materials whose mechanical and physical properties are graded in a specific direction. The gradation direction could be unidirectional, bidirectional, or multidirectional. This smooth

*Corresponding author, Ph.D., E-mail: royalmadan.me@geu.ac.in, royalmadan6293@gmail.com

http://www.techno-press.org/?journal=acd&subpage=7 ISSN: 2383-8477 (Print), 2466-0523 (Online)

transition in material properties can be customized to meet the requirements of various industries and engineering applications (Adiga *et al*. 2022, Ansari *et al*. 2021, Garg *et al*. 2021). This gradual change in microstructure across the interface does not mismatch the mechanical properties across the multiple interfaces as other composite materials, such as laminated reinforced, do Nakamura *et al*. (2000). Such changes in stepwise or continuous gradation in the material result from the fabrication process. To avoid delamination, FGMs provide a gradual variation in microstructure, reducing property mismatches across the interface Suresh and Mortensen (1997).

A bending analysis of functionally graded (FG) rotating disks under various boundary conditions was conducted using a semi-analytical solution. They found that stress induced in an FG disk was lower compared to disks made up of isotropic material (full-metal and full-ceramics) were higher than stresses induced in an FG disk Bayat *et al*. (2009). The developed FGMs can be of stepped or continuously varying types, depending on the fabrication method. The fabrication of FGMs can be carried out by two means: continuous or step-wise. The step-wise layered FGM can be developed using powder metallurgy or additive manufacturing, while a continuous variation in properties can be achieved using the centrifugal casting method Madan and Bhowmick (2020). Unlike laminated composites, which may exhibit abrupt changes in mechanical properties at the interface. FGMs provide a gradual variation in microstructure, reducing property mismatches across the interface (Daneshmand *et al*. 2023, Raad *et al*. 2024). Modeling of FGMs to estimate the material properties is important for the accurate estimation of the field variables. To estimate these properties effectively, two primary approaches are used. The first approach involves determining the volume fraction of the matrix and reinforcement phases using models such as the rule of mixtures, the modified rule of mixtures, the Mori-Tanaka method, and the Halpin-Tsai model (Fallahi Arezodar and Nikbakht 2019, Madan and Bhowmick 2021) The second approach directly assumes material property variations based on predefined functions such as power-law, exponential, or sigmoid distributions. This study follows the latter approach, considering an exponential variation in material properties, including Young's modulus, density, and thermal conductivity, without explicitly accounting for the volume fraction of each phase (Singh *et al*. 2024, Sondhi *et al*. 2023).

In Wang *et al*. (2015), discussed the thermo-mechanical stress analysis and parameter optimization of FG pressure vessels using steady-state thermo-elastic theory with power law material gradation. A problem of stresses induced in an FG hollow cylinder, disk, and sphere under internal pressure is solved using the complementary functions method Tutuncu and Temel (2009). Furthermore, for an FG cylinder under different loading conditions was solved analytically Rahimi *et al*. (2011). For a short hollow cylinder under a steady-state thermal load, stresses are identified analytically Jabbari *et al*. (2009). Elastic analysis of a thick hollow cylinder of variable thickness under arbitrary pressure at the inner surface was performed using finite element analysis Nejad *et al*. (2015). Investigated the thermo-mechanical behavior of various structural components under different loading conditions. Analytical and numerical methods are used, including Hamilton's principle with the extended Kantorovich method for laminated panels Singh and Kumari (2020), a modified bulge test with FEM for MEMS diaphragms was conducted by Altabey (2017) higher-order shear deformation theory with Monte Carlo simulations for functionally graded plates (Achchhe *et al*. (2017). Laplace transformation is applied to analyze nonlocal thermoelastic nanobeams Zenkour and Abouelregal (2018), while a semi-analytical approach is used to study magneto-thermo-elastic effects in piezoelectric hollow spheres Allam *et al*. (2018). These findings offer valuable insights into material behavior under complex conditions, contributing to advancements in engineering design and analysis.

Functionally graded cylinders under extension, torsion, shearing, pressuring, and temperature changes are studied analytically by varying the modulus as per the power law (Tarn 2001). Exact solutions for thermomechanical responses in cylindrically anisotropic functionally graded cylinders under multiple loadings, incorporating radial material variation and rotational effects (Cinefra *et al*. 2010). Thermo-mechanical analysis of FGM cylinders using the smoothed radial point interpolation method (Feng and Li 2017). Analytical and finite element stress analysis of FGM cylinders with exponential property variation is proposed and validated with finite element analysis results (Habib *et al*. 2018). Developed an analytical model for transient thermo-mechanical analysis of FGM thick-walled cylinders using shear deformation theory, the proposed method was validated using FEM and has aerospace and industrial relevance (Vaziri *et al*. 2019). Presented an exact analytical solution for FG thick-walled cylinders under combined thermal and mechanical loads, validated by FEM (Das *et al*. 2024). Investigates the nonlinear vibration behavior of functionally graded cylindrical shells reinforced with eccentrically placed stiffeners under thermo-mechanical loading. Using analytical and numerical methods, they found that increasing foundation stiffness increases the natural frequencies, while higher temperatures reduce frequencies and structural rigidity, demonstrating the coupled thermo-mechanical effects on dynamic performance (Muthanna *et al*. 2025). Analyzed the nonlinear free vibration of porous functionally graded sandwich plates under hygrothermal conditions using FSDT and Hamilton's principle. They illustrate how porosity, hygrothermal effects, and geometry influence the natural frequencies. The results are validated with FEM and found a maximum 11% discrepancy from analytical results (Alhous *et al*. 2025). The gradation variation structures like beam, plate, shell (Abbas *et al*. 2025) and sandwich structures (Njim *et al*. 2021, 2024) can be unidirectional (Hadji *et al*. 2021, Viet *et al*. 2020), bidirectional (Lu and Chen 2020) or multidirectional (Hadji *et al*. 2024a, b). During the fabrication of FGM, porosity develops. To analyze the behavior of the structure for various porosity distributions, extensive research has been conducted (Hadji *et al*. 2023, Kadum Njim *et al*. 2024, Madan *et al*. 2023, Raad *et al*. 2024). To avoid the development of porosities, the process parameters, such as sintering temperature, holding time and temperature, compaction load, scan rate, and melting temperature, need to be optimized (Hangai *et al*. 2016, Madan and Bhowmick 2022).

From a host of literature, till date, no research has been identified that focuses on developing an analytical solution for the thermo-mechanical deformation and stress analysis of functionally graded cylindrical vessels subjected to a combination of angular rotations, body force, mechanical loads, and thermal loads with heat generation. The mechanical loads include both internal and external pressure, while the thermal loads account for the effects of heat conduction and internal heat generation within the material. Understanding the behavior of these vessels under such conditions is crucial, particularly for applications in aerospace, nuclear reactors, and pressure vessel industries, where functionally graded materials (FGMs) offer superior performance due to their spatially varying properties. Moreover, real-life loading conditions often involve a complex interplay of multiple forces, yet no existing study systematically examines the stress and deformation response of functionally graded cylindrical vessels under such conditions. Investigating the impact of material parameters following a power-law variation, along with the effects of thermal and mechanical loading parameters and body forces, is essential to gain deeper insights into their structural behavior. This method allows for an accurate analytical evaluation of the stress and deformation distribution, offering valuable insights into the performance and reliability of functionally graded cylindrical vessels under diverse operating conditions.

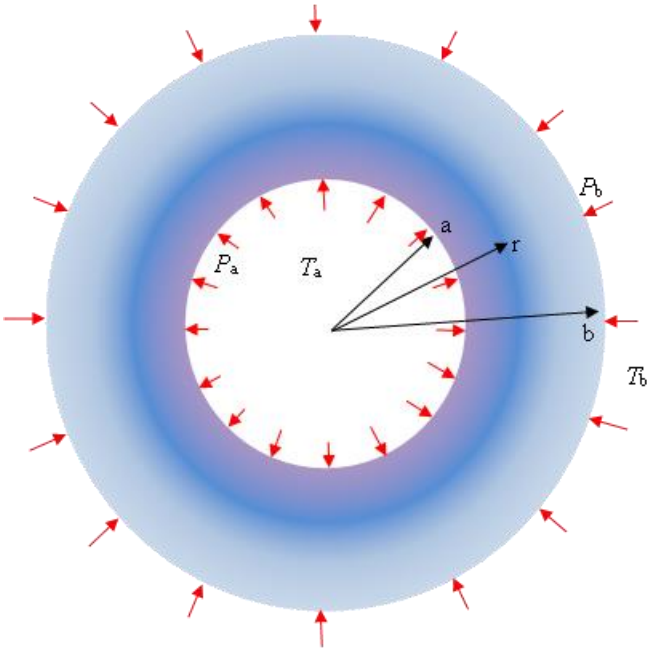

Fig. 1 FGM cylinder

2. Mathematical formulation

Considering a hollow cylindrical geometry made of FG material with inner radius ***a*** and outer radius ***b*** as shown in Fig. 1. Let the displacement 'u' be the function of the radius of a cylinder. The radial strain, tangential strain, and displacement are related as Eq. 1 Jabbari *et al*. (2002):

$$\varepsilon_{rr} = \frac{du}{dr} = \frac{1}{Y_{rr}}[\sigma_{rr} - \vartheta\sigma_{tt}] + \varepsilon_{tt}{}^{*}\,,\ \varepsilon_{tt} = \frac{u}{r} = \frac{1}{Y_{rr}}[\sigma_{tt} - \vartheta\sigma_{rr}] + \varepsilon_{tt}{}^{*}\,,\ \varepsilon_{tt}{}^{*} = \alpha_{rr}T_{rr} \qquad (1)$$

Plane stress state is considered for reducing the complexity of the analysis, in plane stress condition, the thickness of the cylinder wall is very thin as compared to the radius. For elastic materials, the thermo-mechanical stress-strain relations for non-homogeneous and isotropic materials under the influence of temperature are given by Hook's law Sondhi *et al*. (2024):

$$\sigma_{rr} = Y_{rr}\lambda[\varepsilon_{rr}(1-\vartheta) + \vartheta\varepsilon_{tt} - (1+\vartheta)\varepsilon_{rr}{}^{*}]\,,\ \sigma_{tt} = Y_{rr}\lambda[\vartheta\varepsilon_{rr} + (1-\vartheta)\varepsilon_{tt} - (1+\vartheta)\varepsilon_{rr}{}^{*}] \quad (2)$$

where, Y_{rr} is Young's modulus at radius r, λ is lame constant, ϑ is considered the constant Poisson's ratio.

Eq. (3) shows the governing equilibrium equation expressed by Navier's equation for the plane stress, including the body force and the inertia term in the radial direction. The basic unknown parameter is the displacement at each discretised point along the thickness of the cylinder.

$$r\frac{d}{dr}\sigma_{rr} + \left(\sigma_{rr} - \sigma_{t_t}\right) + \rho_{rr}\left(\omega^2 - \frac{g}{a}\right)r^2 = 0 \qquad (3)$$

The material properties assumed to vary as follows (Avcar 2019, Eraslan and Orcan 2002):

$$E_{rr} = E_a(r)^{m_1},\ \alpha_{rr} = \alpha_a(r)^{m_2},\ k_{rr} = k_a(r)^{m_3}$$
$$\rho_{rr} = \rho_a(r)^{m_4},\ q_{rr} = q_a(r)^{m_5} \tag{4}$$

To solve the governing equation, the first strains, which are a function of displacement as in Eq. (1), are substituted into the stress-strain relation as in Eq. (2), illustrating the stress as a function of displacement. Then the results are substituted in governing differential Eq. (3), and finally, the Navier's equation in the form of displacement is found,

$$\begin{aligned} & r\frac{d}{dr}\left[E_{rr}\lambda\left\{(1-\vartheta)\frac{du}{dr}+\vartheta\frac{u}{r}-(1+\vartheta)\alpha_{rr}T_{rr}\right\}\right] \\ & +E_{rr}\lambda\left[(1-\vartheta)\frac{du}{dr}+\vartheta\frac{u}{r}-(1+\vartheta)\alpha_{rr}T_{rr}\right] \\ & -E_{rr}\lambda\left[\vartheta\frac{du}{dr}+(1-\vartheta)\frac{u}{r}-(1+\vartheta)\alpha_{rr}T_{rr}\right] \\ & +\rho_{rr}(\omega^2-\frac{g}{a})r^2=0 \end{aligned} \tag{5}$$

where,

$$\lambda = \frac{1}{(1+\vartheta)(1-2\vartheta)} \tag{6}$$

For ease of the calculation, Eq. (5) can be rewritten and converted into standard differential equation form and introducing some arbitrary constants as,

$$Ar^2\left(\frac{d^2u}{dr^2}\right)+Br\left(\frac{du}{dr}\right)+C(u)=Ur^{m_2+P_4+1}+Vr^{m_2-m_3+m_5+3}+Wr^{m_2+1}+Sr^{m_4-m_1+3} \tag{7}$$

where,

$$\begin{aligned} A &= E_a\lambda(1-\vartheta),\ B = E_a\lambda[m_1(1-\vartheta)+(1-\vartheta)], \\ C &= E_a\lambda(\vartheta m_1+\vartheta-1)U=\tfrac{1}{(1-2\vartheta)}E_a\alpha_aQ_4[P_4+m_1+m_2], \\ V &= \frac{\beta_1E_a\alpha_a}{(1-2\vartheta)}[m_5-m_3+m_1+m_2+2] \\ W &= \tfrac{E_a\alpha_aQ_3}{(1-2\vartheta)}[m_1+m_2], S=-\rho_a\left[\omega^2-\left(\tfrac{g}{a}\right)\right] \end{aligned} \tag{8}$$

3. Temperature formulation

Assuming FG materials under high-temperature application, combinations of material properties will be chosen based on temperature. The temperature distribution of a one-dimensional steady-state heat conduction equation with constant heat flux is governed by varying heat conductivity Reddy and Chin (1998).

$$\frac{1}{r}\frac{d}{dr}\left[rk_{rr}\frac{d}{dr}T_{rr}\right]+q_{rr}=0 \tag{9}$$

The thermal boundary conditions employed at the inner and outer radius of a cylinder are given by Eq. (10),

where, T_{rr} is the temperature at any radius, the temperature at the inner and outer radius was defined by $T_a \& T_b$.

Differentiating the above Eq. (9), the Navier's equation for temperature can be written as:

$$T_{rr}|r = a = T_a \text{ and } T_{rr}|r = b = T_b \tag{10}$$

$$A_1 r^2 \left(\frac{d^2 T_{rr}}{dr^2}\right) + B_1 r \left(\frac{dT_{rr}}{dr}\right) + C_1(T_{rr}) = \gamma_1 r^{m_5 - m_3 + 2} \tag{11}$$

where,

$$A_1 = k_a,\ B_1 = k_a(1 + m_3),\ C_1 = 0,\ \gamma_1 = -q_a,\ P_3 = 0, P_4 = \left(\frac{A_1 - B_1}{A_1}\right) = -m_3 \tag{12}$$

$$\frac{dT_{rr}}{dr} = P_4 Q_4 r^{P_4 - 1} + \beta_1(m_5 - m_3 + 2) r^{m_5 - m_3 + 1} \tag{13}$$

$$T_{rr} = Q_3 + Q_4 r^{P_4} + \beta_1 r^{m_5 - m_3 + 2} \tag{14}$$

Solving for Q_3 and Q_4 yields

$$Q_4 = \frac{T_a - T_b}{a^{P_4} - b^{P_4}} - \frac{\beta_1(a^{m_5 - m_3 + 2} - b^{m_5 - m_3 + 2})}{a^{P_4} - b^{P_4}},\ Q_3 = T_a - \beta_1 a^{m_5 - m_3 + 2} - Q_4 a^{P_4} \tag{15}$$

4. Solution of displacement Equation

The Navier's equation for radial displacement 'u' is given in Eq. (7), the aforementioned equation is a non-homogeneous Euler differential equation, which is solved in 2 sections: a. general solution (u_g) using homogeneous part and b. particular solution using the non-homogeneous part Vasil'ev and Fedorov (2022)

$$u_g = Q r^P \tag{16}$$

Substitute the above Eq. (16) in the homogeneous Eq. (7)

$$AP^2 + (B - A)P + C = 0 \tag{17}$$

The above Eq. (17) has 2 real roots P_1 and P_2, which are given by

$$P_{1,2} = \frac{(A - B) \pm \sqrt{(B - A)^2 - 4AC}}{2A} \tag{18}$$

Thus, the general solution is

$$u_g(r) = Q_1 r^{P_1} + Q_2 r^{P_2} \tag{19}$$

Now particular part of solution u_p is assuming to have the form

$$u_p = I r^{m_2 + P_4 + 1} + J r^{m_2 - m_3 + m_5 + 3} + L r^{m_2 + 1} + M r^{m_4 - m_1 + 3} \tag{20}$$

Substitute above Eq. (20) in Eq. (7) then rearrange, we get,

$$\begin{bmatrix}A(m_2+P_4+1)(m_2+P_4)+\\B(m_2+P_4+1)+C\end{bmatrix}Ir^{m_2+P_4+1}$$
$$+\begin{bmatrix}A(m_2+m_5-m_3+3)(m_2+m_5-m_3+2)\\+B(m_2+m_5-m_3+3)+C\end{bmatrix}Jr^{m_2-m_3+m_5+3}$$
$$+[A(m_2+1)m_2+B(m_2+1)+C]Lr^{m_2+1}+$$
$$\begin{bmatrix}A(m_4-m_1+3)(m_4-m_1+2)+\\B(m_4-m_1+3)+C\end{bmatrix}Mr^{m_4-m_1+3}$$
$$=Ur^{m_2+P_4+1}+Vr^{m_2-m_3+m_5+3}+Wr^{m_2+1}+Sr^{m_4-m_1+3} \tag{21}$$

$$I=\frac{U}{A[(m_2+P_4+1)(m_2+P_4)]+B[m_2+P_4+1]+C}$$
$$J=\frac{V}{\begin{bmatrix}A\{(m_2+m_5-m_3+3)(m_2+m_5-m_3+2)\}\\+B(m_2-m_3+m_5+3)+C\end{bmatrix}}$$
$$L=\frac{W}{A[(m_2+1)(m_2)]+B[(m_2+1)]+C} \tag{22}$$
$$M=\frac{S}{\begin{bmatrix}A[(m_4-m_1+3)(m_4-m_1+2)]\\+B[(m_4-m_1+3)]+C\end{bmatrix}}$$

Equating the coefficient of identical power we have:

Now, the complete solution for u is the sum of general solution and particular solution as,

$$u=u_g+u_p \tag{23}$$

Thus,

$$u=Q_1r^{P_1}+Q_2r^{P_2}+Ir^{m_2+P_4+1}+Jr^{m_2+m_5-m_3+3}+Lr^{m_2+1}+Mr^{m_2-m_1+3} \tag{24}$$

Substituting Eq. (24) in Eq. (1) to (4), the strains distributions and stresses distributions are obtained as,

$$\varepsilon_{rr}=Q_1P_1r^{P_1-1}+Q_2P_2r^{P_2-1}+I(m_2+P_4+1)r^{m_2+P_4+1}$$
$$+J(m_2-m_3+m_5+3)r^{m_2-m_3+m_5+2}+L(m_2+1)r^{m_2}+M(m_4-m_1+3)r^{m_4-m_1+2} \tag{25}$$

$$\varepsilon_{tt}=Q_1r^{P_1-1}+Q_2r^{P_2-1}+Ir^{m_2+P_4}+Jr^{m_2-m_3+m_5+2}+Lr^{m_2}+Mr^{m_4-m_1+2} \tag{26}$$

$$\sigma_{rr}=E_a\lambda\begin{bmatrix}Q_1\{(1-\vartheta)P_1+\vartheta\}r^{m_1+P_1-1}+\\Q_2\{(1-\vartheta)P_2+\vartheta\}r^{m_1+P_2-1}\\+Ir^{m_1+m_2+P_4}\{(1-\vartheta)(m_2+P_4+1)+\vartheta\}+\\Jr^{m_1+m_2+m_5-m_3+2}\{(1-\vartheta)(m_2+m_5-m_3+3)+\vartheta\}\\+Lr^{m_1+m_2}\{(1-\vartheta)(m_2+1)+\vartheta\}+\\Mr^{m_4+2}\{(1-\vartheta)(m_4-m_1+3)+\vartheta\}\\-(1+\vartheta)\alpha_a\begin{Bmatrix}Q_3r^{m_1+m_2}+Q_4r^{m_1+m_2+P_4}+\\\beta_1r^{m_1+m_2+m_5-m_3+2}\end{Bmatrix}\end{bmatrix} \tag{27}$$

Q_1 and Q_2 are determined using the mechanical free-free boundary conditions, considering the internal pressure p_a and external pressure p_b

$$\sigma_{rr} = -p_a \text{ and } \sigma_{rr} = -p_b \tag{28}$$

Substituting the mechanical boundary condition, eq. (28) in Eq. (27), the constants become

$$Q_2 = \frac{\phi_{22}X - \phi_{21}Y}{\phi_{11}\phi_{22} - \phi_{12}\phi_{21}}, \qquad Q_2 = \frac{\phi_{11}Y - \phi_{21}X}{\phi_{11}\phi_{22} - \phi_{12}\phi_{21}} \tag{29}$$

where,

$$\begin{aligned}
\phi_{11} &= E_a\lambda[P_1(1-\nu)+\nu]a^{m_1+P_1-1} \\
\phi_{12} &= E_a\lambda[P_2(1-\nu)+\nu]a^{m_1+P_2-1} \\
\phi_{21} &= E_a\lambda[P_1(1-\nu)+\nu]b^{m_1+P_1-1} \\
\phi_{22} &= E_a\lambda[P_2(1-\nu)+\nu]b^{m_1+P_2-1}
\end{aligned} \tag{30}$$

$$X = -Z(a) - p_a \ , \quad Y = -Z(b) - p_b \tag{31}$$

$$Z(a) = E_a\lambda\begin{bmatrix} Q_1\{(1-\vartheta)P_1+\vartheta\}a^{m_1+P_1-1} + \\ Q_2\{(1-\vartheta)P_2+\vartheta\}a^{m_1+P_2-1} \\ +Ia^{m_1+m_2+P_4}\{(1-\vartheta)(m_2+P_4+1)+\vartheta\} + \\ Ja^{m_1+m_2+m_5-m_3+2}\{(1-\vartheta)(m_2+m_5-m_3+3)+\vartheta\} \\ +La^{m_1+m_2}\{(1-\vartheta)(m_2+1)+\vartheta\} + \\ Ma^{m_4+2}\{(1-\vartheta)(m_4-m_1+3)+\vartheta\} \\ -(1+\vartheta)\alpha_a\begin{Bmatrix} Q_3a^{m_1+m_2} + Q_4a^{m_1+m_2+P_4} + \\ \beta_1a^{m_1+m_2+m_5-m_3+2} \end{Bmatrix} \end{bmatrix} \tag{32}$$

$$Z(b) = E_a\lambda\begin{bmatrix} Q_1\{(1-\vartheta)P_1+\vartheta\}b^{m_1+P_1-1} + \\ Q_2\{(1-\vartheta)P_2+\vartheta\}b^{m_1+P_2-1} \\ +Ib^{m_1+m_2+P_4}\{(1-\vartheta)(m_2+P_4+1)+\vartheta\} + \\ Jb^{m_1+m_2+m_5-m_3+2}\{(1-\vartheta)(m_2+m_5-m_3+3)+\vartheta\} \\ +Lb^{m_1+m_2}\{(1-\vartheta)(m_2+1)+\vartheta\} + \\ Mb^{m_4+2}\{(1-\vartheta)(m_4-m_1+3)+\vartheta\} \\ -(1+\vartheta)\alpha_a\begin{Bmatrix} Q_3b^{m_1+m_2} + Q_4b^{m_1+m_2+P_4} + \\ \beta_1b^{m_1+m_2+m_5-m_3+2} \end{Bmatrix} \end{bmatrix} \tag{33}$$

5. Results and discussion

Thermo-mechanical stress analysis was carried out on a functionally graded hollow cylindrical vessel subjected to varying thermal distribution. FGM-composed results are presented and assumed to be temperature-independent, isotropic elastic material properties. The geometrical and mechanical properties are given in Table 1. Displacement, stress, and material properties along the radial direction of the cylinder are represented as dimensionless values to demonstrate the effect of

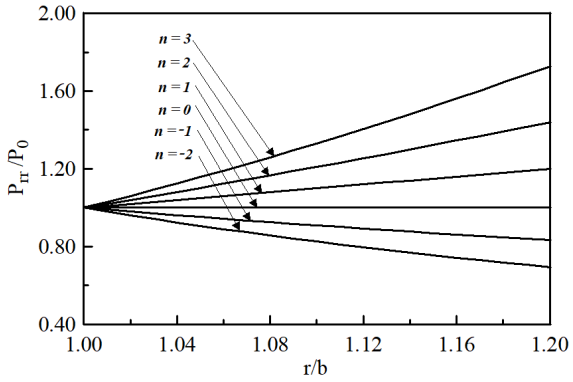

Fig. 2 Material property variation

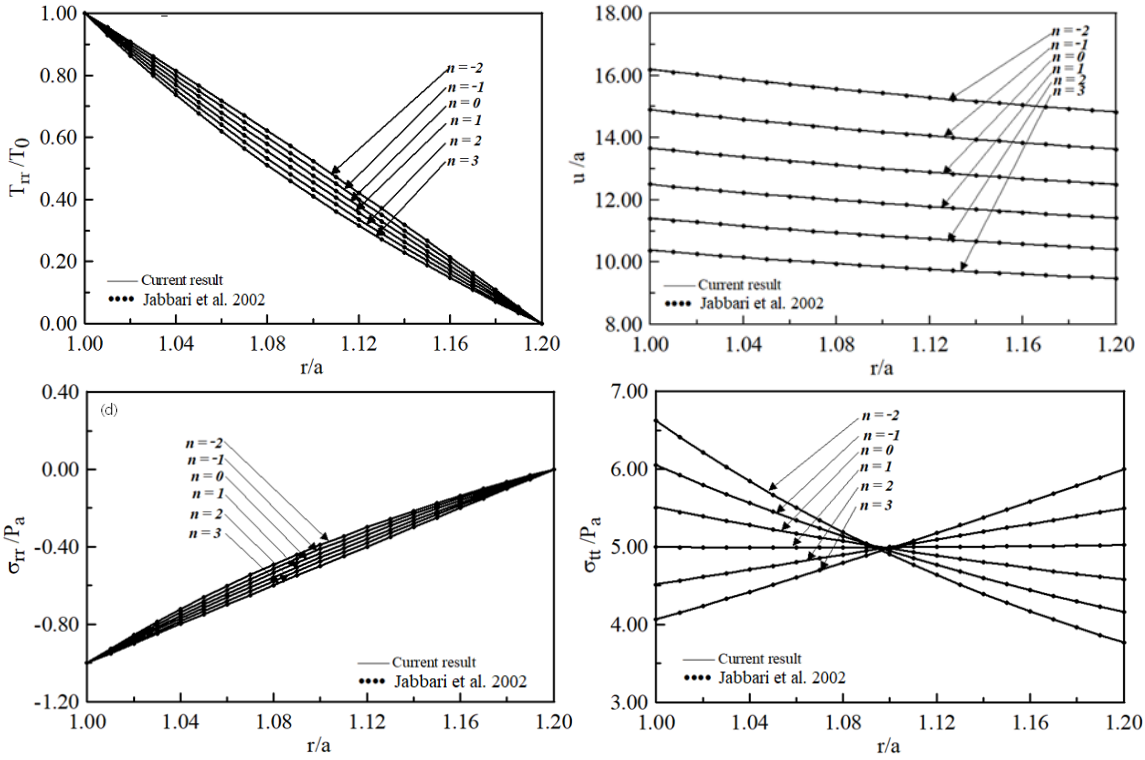

Fig. 3 (a)-(d) Validation plot

the FG material. The following dimensionless values were used for the presentation of numerical results: $P = \frac{P_{rr}}{P_0}$, $\sigma_r{}^* = \frac{\sigma_{rr}}{\sigma_0}$, $\sigma_\theta = \frac{\sigma_{\theta\theta}}{\sigma_0}$, $u^* = \frac{u}{b}$

5.1 Material properties

Fig. 2 represents the dimensionless elastic modulus, thermal expansion coefficient, thermal conduction coefficient, and density, where $m_1 = m_2 = m_3 = m_4 = n$ and $m_5 = 0$ for constant

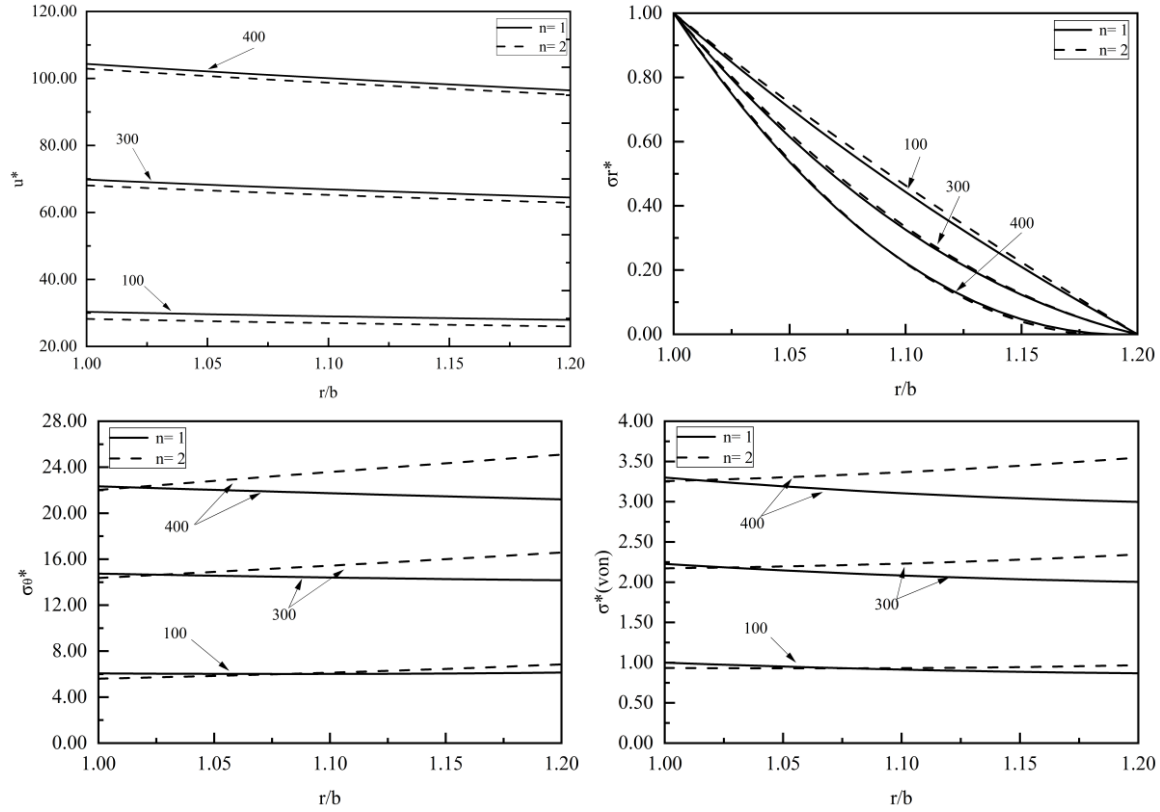

Fig. 4 Effect of various rotations (internal pressure) on displacement and stresses (radial, tangential and von Mises)

heat flux along the radius. The inhomogeneity constant shows the stiffness variation along the radius, i.e., n > 0 means increasing the stiffness and ***n*** < 0 means decreasing the stiffness in the radial direction. An ***n*** = 0, shows the isotropic material properties.

5.2 Validation of the present study

The present approach was validated with Jabbari *et al*. (2002) to check the feasibility of the methodology, which is illustrated in Fig. 3(a-d). Illustrated figures show excellent agreement with the literature. For the effective stress analysis, the von Mises stress distribution $\sigma * = \sqrt{2}|\sigma_{rr} - \sigma_{tt}|$ is analyzed for all cases.

5.3 Effect of various rotations (internal pressure)

The radial displacement and stress, such as radial, tangential, and von Mises, are represented by Fig. 4, for the various angular rotations (100, 300, 400) with internally pressurized (50 MPa) mechanical loading conditions. Displacement and stresses (tangential & von Mises) are directly related to the angular rotation in both ***n*** = 1 & 2, i.e., angular rotation helps to increase the loading condition, due to this increment in loading, the displacement and stresses also increase. But the

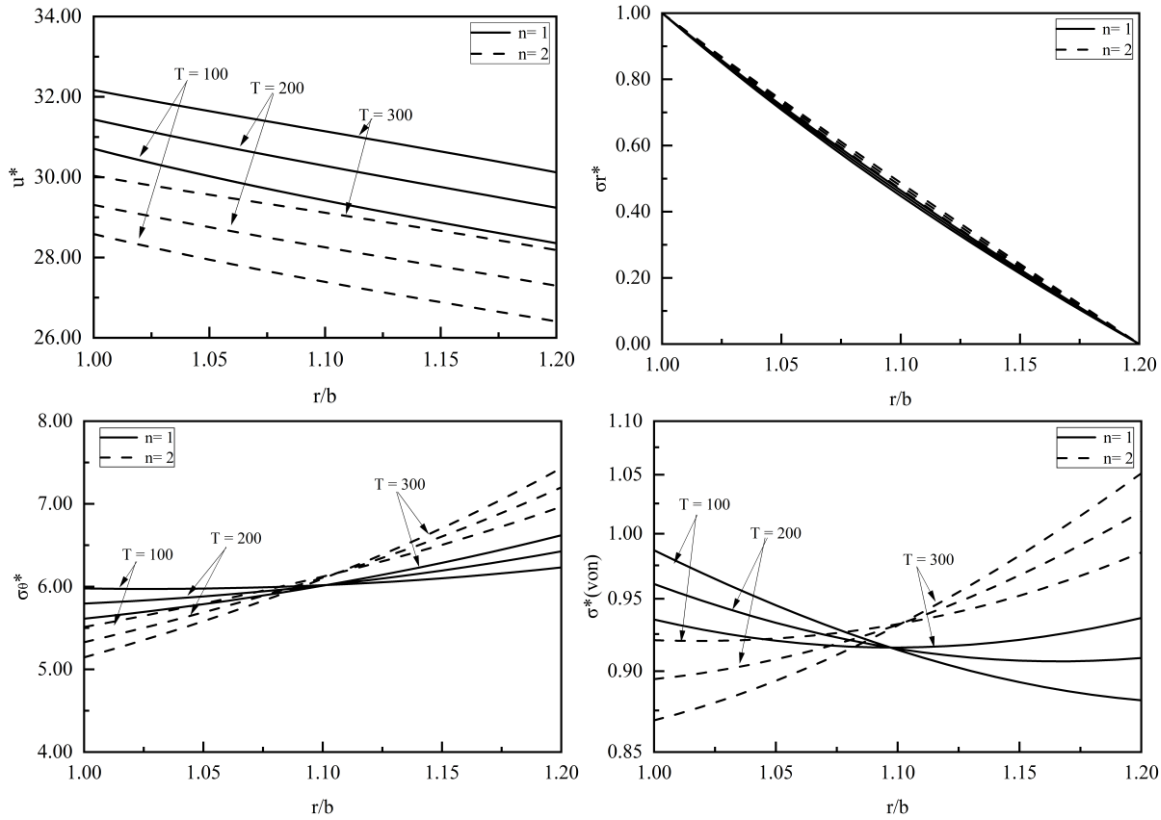

Fig. 5 Effect of various temperature (internal pressure) on displacement and stresses (radial, tangenti al and von Mises)

radial stress behaves in inverse relation to angular rotation, because the inner region resists internal pressure, experiencing compressive radial stress, while at the outer region tensile stress is generated, which is the dominating stress. The von Mises stress distribution shows the cumulative effect of radial and tangential stress, which is more influenced by the tangential stress as shown. For accurate prediction of failure, it is essential to thoroughly understand the stress variation with varying angular rotation & material properties.

5.4 Effect of various temperatures (internal pressure)

The effect of various temperatures (100, 200, 300) with internal pressure (50 MPa) on displacement and stress (radial, tangential, and von Mises) is shown in Fig. 5, respectively. The displacement and radial stress are illustrating the direct relation with the temperature as shown in Fig. 5 for both $\boldsymbol{n}$ = 1 & 2, because increasing the temperature softens the material that influences and reduces the radial stress and increases radial deformation. On the other hand, the tangential and von Mises stresses are inversely related to temperature till the ratio $\boldsymbol{r/b}$ = 1.08, beyond this, the relationship becomes proportional because after a certain value of radius, the temperature is less pronounced due to thus the dominant effect is less. Beyond the critical radius, the tangential stress is more influenced by temperature, resulting in higher tangential and von Mises stress.

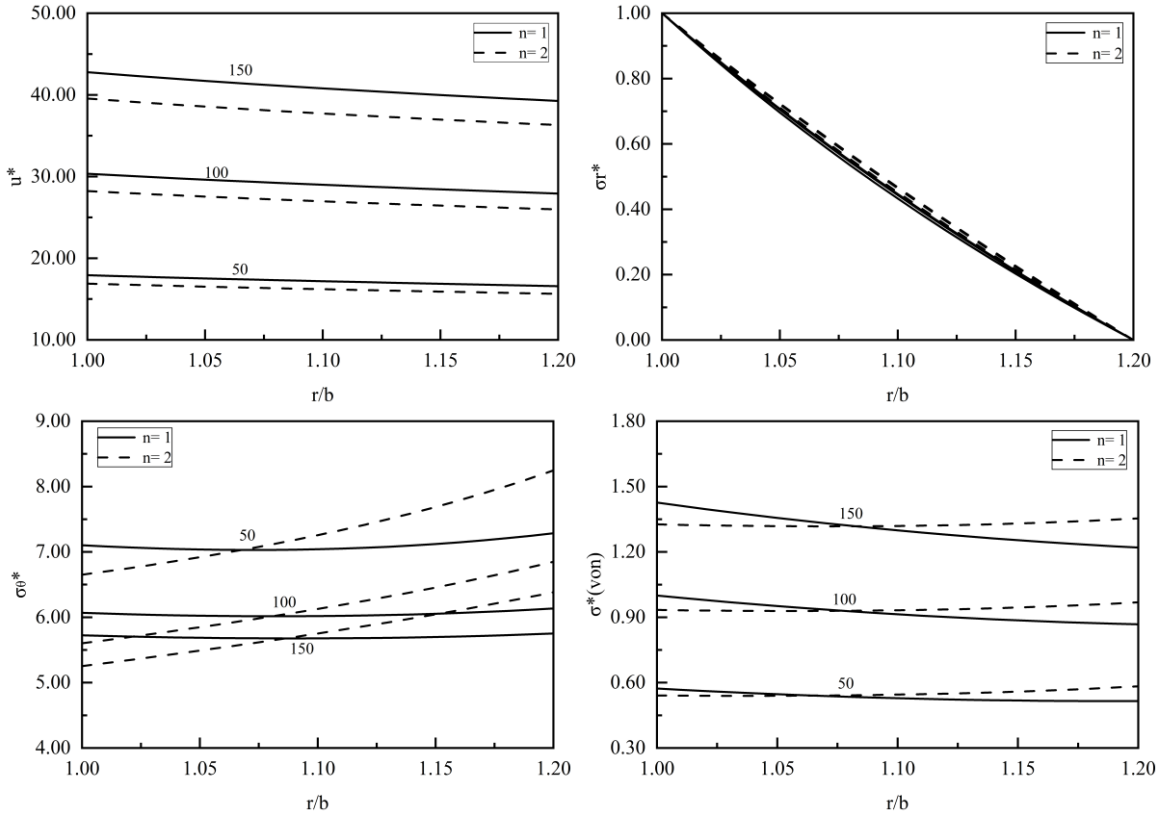

Fig. 6 Effect of various pressures (internal pressure) on displacement and stresses (radial, tangential, and von Mises)

5.5 Effect of various pressures (internal pressure)

The influence of various internal pressures (50, 100, 150 MPa) on radial displacement and stresses such as radial, tangential, and von Mises, is shown in Fig. 6, respectively. These variations in internal pressure directly influence the radial displacement, radial stress, and von Mises stress, with a higher magnitude at the inner surface and lowest at the outer surface, which represents the linear elastic behavior where stress is directly proportional to the strain. But in the case of tangential stress, the relation with internal pressure is opposite, with a higher magnitude at the outer surface as compared to the inner surface. An increase in pressure leads to radial expansion radially which decreases the tangential stress. This critical response is important to understand the failure modes under various pressures.

5.6 Effect of various rotations (external pressure)

In this case, the influence of various rotations (100, 300, 400) under external pressure (100 MPa) is considered to analyze the radial displacement and stresses (radial, tangential, and von Mises) of the FG cylinder as shown in Fig. 7, respectively. Radial displacement and tangential stresses are directly influenced by angular rotation because centrifugal force becomes more

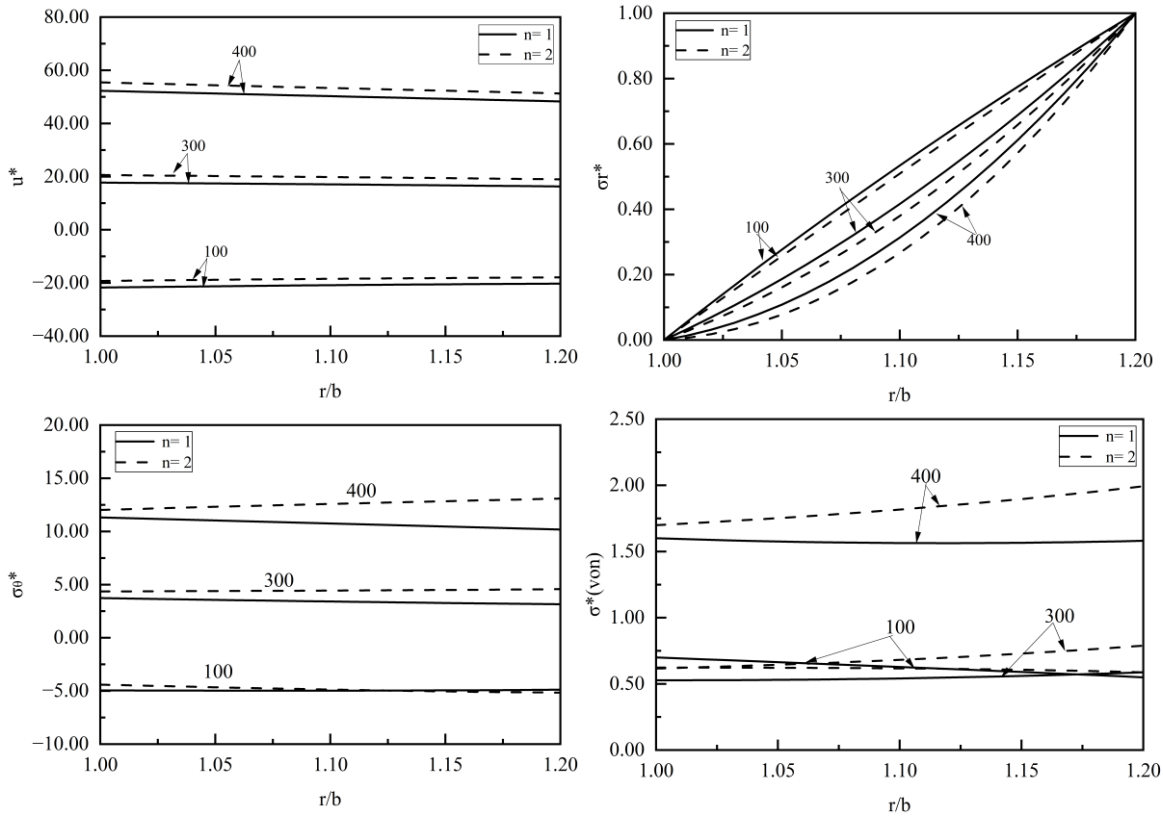

Fig. 7 Effect of various rotations (external pressure) on displacement and stresses (radial, tangential, and von Mises)

dominant with an increase in angular rotation. This reduces the net compressive force due to the external pressure and results outward expansion of walls. However, radial stress shows a non-linear inverse response. While compressive radial stress due to external pressure opposes the outward centrifugal force and reduces the compressive effects. This leads to lower radial stress magnitude as the angular velocity increases. The von Mises stress variation shows the complex pattern due to conflict behaviour between tangential and radial stresses, due to this, it is necessary to individually analyse both the components for failure prediction.

5.7 Effect of various temperatures (external pressure)

In this case, the effect of various temperatures (100, 200, 300) with external pressure (100 MPa) is considered for the analysis and represented in Figs. 8, respectively. The radial stress is directly influenced because it is the ability of the material (thermal expansion) to resist radial pressure (compressive) that leads to the radial stress by stiffening the inner layers under thermal gradient. Whereas the radial displacement varies inversely with temperature and external pressure case because when increasing the temperature, material generally expands, but external pressure exhibits compression. The material leading to less resistance against displacement due to the combined effect those results in it being more easily deformable. Tangential stress and von Mises

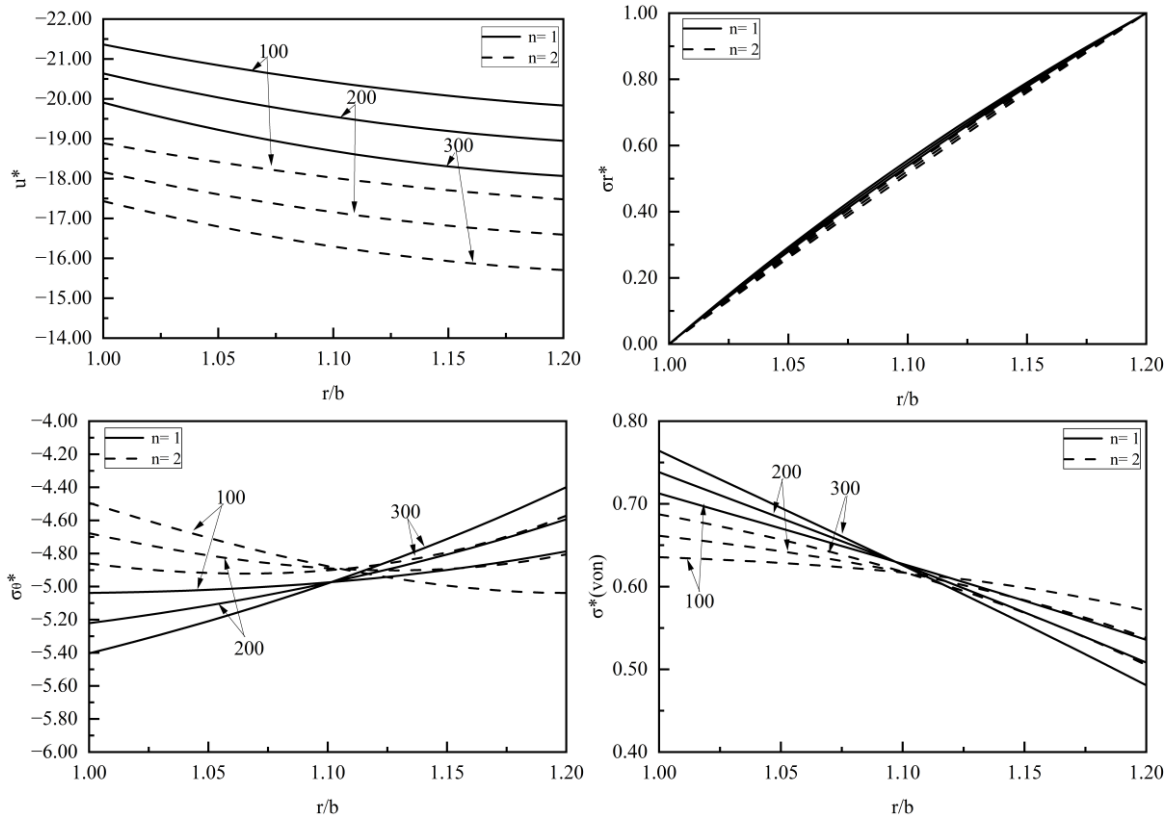

Fig. 8 Effect of various temperatures (external pressure) on displacement and stresses (radial, tangential, and von Mises)

stresses are converging & directly influenced up to ***r/b*** = 1.10, then diverging onwards. At this critical point, the outer layer of wall material becomes softer due to the thermal effect and becomes dominant than the compressive force. In this region material easily deforms and the tangential and von-Mises stresses pattern changes.

5.8 Effect of various pressures (external pressure)

In this scenario, various external pressures (50, 100, 150 MPa) are considered for the analysis of radial displacement and stress, as shown in figs. 9, respectively. As expected, the magnitude of displacement and stress is directly influenced by the external pressure. Because an increase in external pressure imposed higher compressive forces. This proportional relation is also justified by the classical mechanics principles that material behaves elastically under a specified pressure range. Critical tangential stress in between different grading indices is decreasing while increasing the external pressure, but the critical von Mises stress between grading indices increases with an increase in the external pressure because stiffer materials resist radial expansion effectively, and alter the stress components. The material yielding is more pronounced in the case of increasing external pressure.

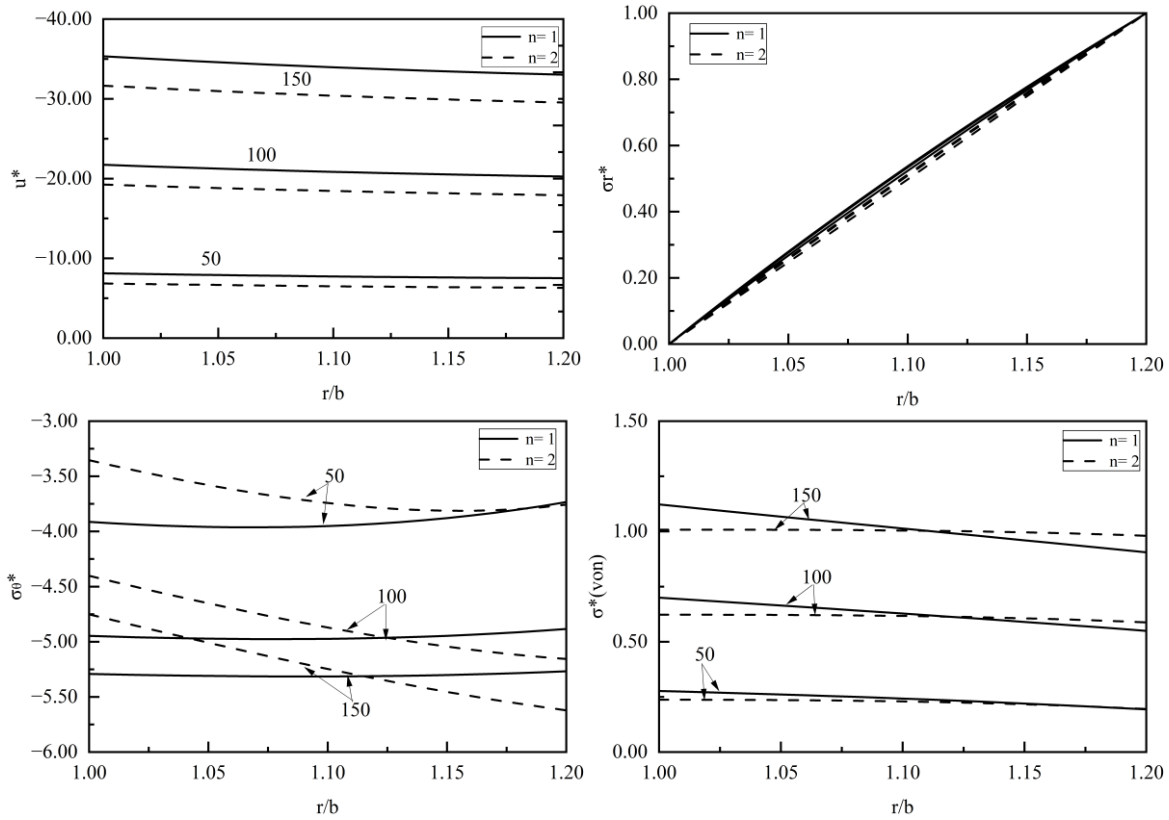

Fig. 9 Effect of various pressures (external pressure) on displacement and stresses (radial, tangential and von Mises)

5.9 Effect of various rotations (internal and external pressure)

In this case, the combined loading condition of various angular rotations (50, 100, 150) under both internal (50 MPa) & external (100 MPa) pressure is analysed. As the radial displacement and tangential stresses are directly proportional to the loading condition considered in this case, with a slightly higher magnitude at the inner surface because a higher value of angular rotation generates higher centrifugal forces. In contrast, radial stress is inversely proportional to the mechanical and centrifugal loading conditions because the compressive force of external and internal pressures is reduced due to the increase in centrifugal force that creates conflicting behaviors of the von Mises distribution as shown in Fig. 10(a-d), leads to non-monotonic von-Mises stress distribution. These complex stress fields require careful evaluation to avoid material failure an unexpected region.

5.10 Effect of various temperatures (internal and external pressure)

This case study explains the effect of various temperatures (50, 100, 150) under internal (50 MPa) & external (100 MPa) pressure on displacement and stresses as shown in Fig. 11 (a-d), respectively. Radial displacement shows an inverse relation to thermal loading conditions because although materials tend to expand with heat, the net mechanical load is compressive, which

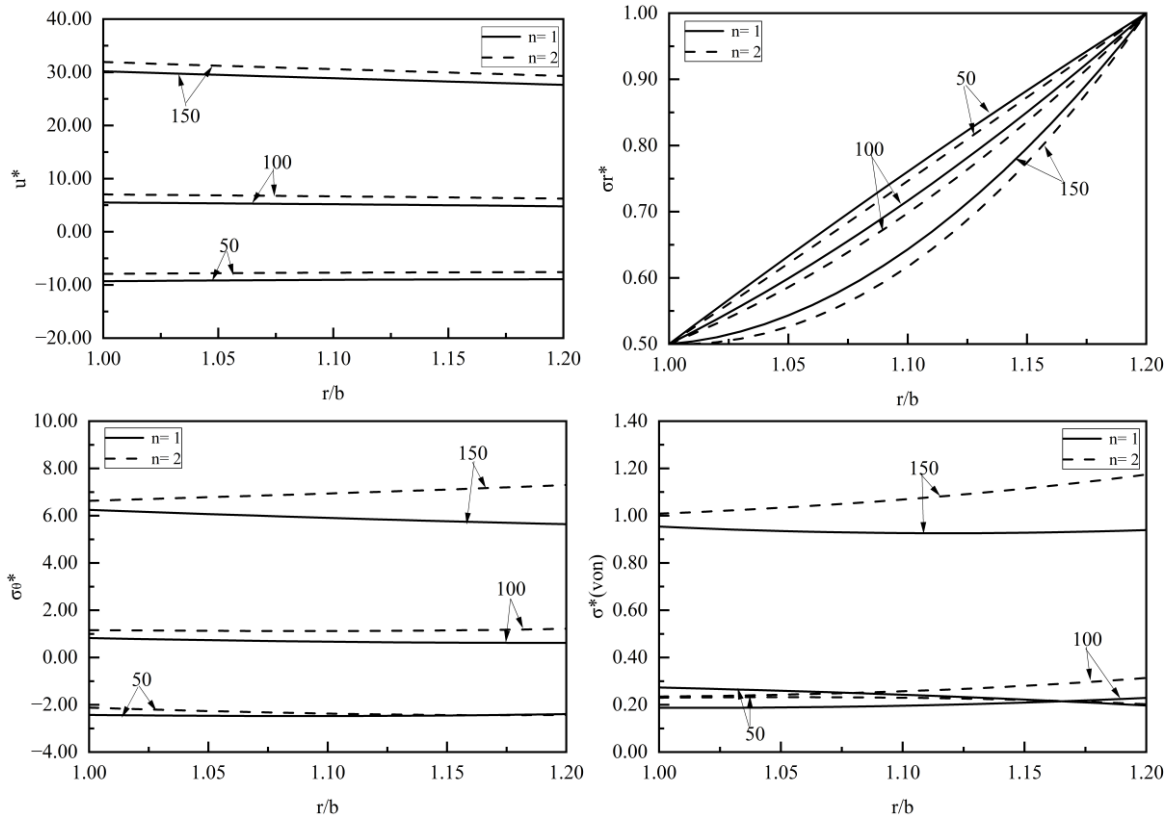

Fig. 10 Effect of various rotations (internal and external pressure) on displacement and stresses (radial, tangential and von Mises)

dominates at elevated temperatures. Whereas radial stress is directly proportional to temperature, because the ability of the material to withstand radial stress is increased with temperature rise, also material's ability to resist compressive force due to pressure is better at higher temperatures due to a softer outer region and a stiffer inner region. Tangential and von Mises stresses are increasing up to a critical radius, and beyond inverse trend follows. This is because the material's response is more uniform near the inner region, whereas the outer region may experience different responses as compared to the inner region. The converging-to-diverging behavior is caused by thermal softening in the outer wall of the structure. This complex scenario must be accounted for in designing high-temperature pressure vessel.

5.11 Effect of various pressures (internal and external pressure)

Finally, in this section, the effect of various internal (100, 200, and 300 MPa) and constant external (100 MPa) pressures is considered for analysis. It is found that the directly proportional relationship of radial displacement, tangential stress, and von Mises stress with the loading condition is due to the dominating internal expansion force. Also indicates that an increase in elastic deformation leads to more noticeable responses. However, radial stress is inversely related to loading conditions because the outward centrifugal force is balanced by the compression force.

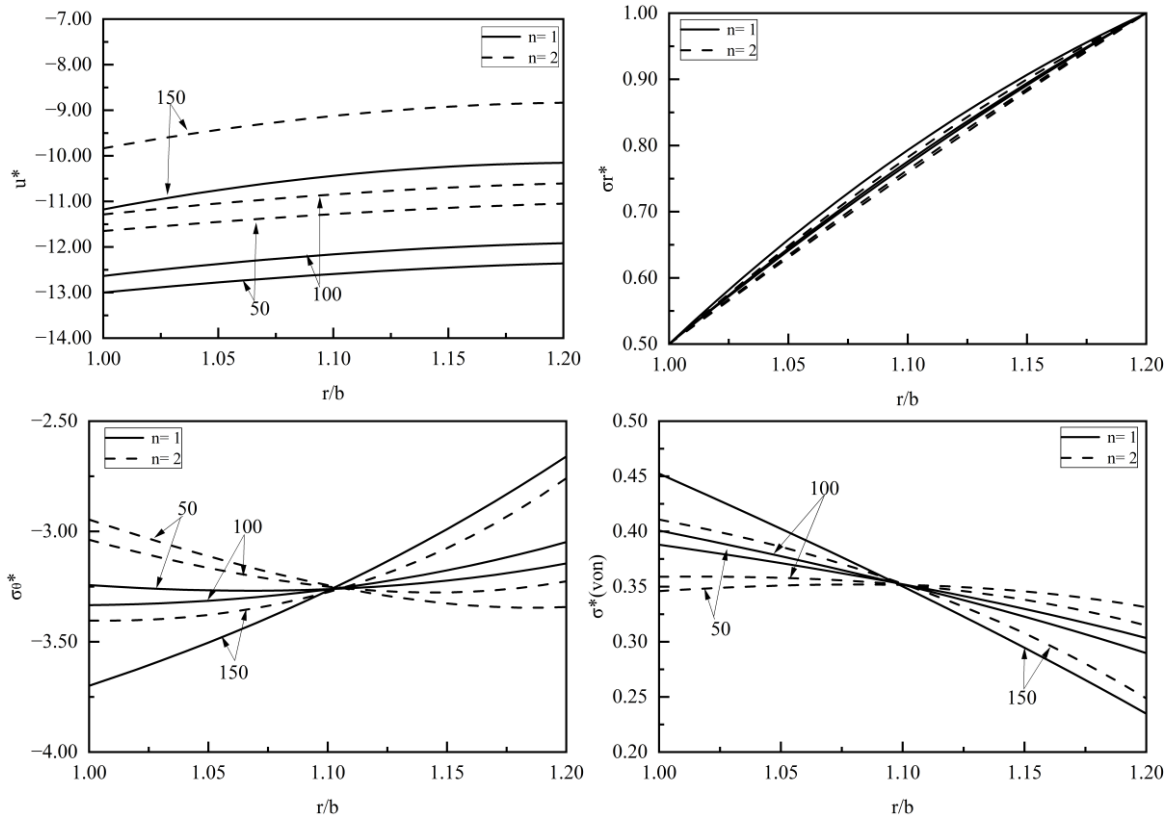

Fig. 11 Effect of various temperatures (internal and external pressure) on displacement and stresses (radial, tangential, and von Mises)

Also, the critical stress for different grading index shifts outward when increasing the pressure loading, indicating that the dominating tensile effect is due to higher pressure and stiffer outer materials can bear higher stress. Meanwhile, maximum von-Mises stress is shifting inward, indicating that a more complex interaction between radial and tangential stress components. This important insight is useful for optimum design against failure.

6. Conclusions

In this study, an exact thermo-mechanical analytical solution for an FG cylindrical pressure vessel has been presented by assuming the varying material properties and a constant Poisson's ratio. Different cases of loading are considered as described in the above sections. Thermo-mechanical elastic stresses for free-free boundary conditions were obtained. The effect of non-homogeneity constant, angular rotation, varying temperature, and internal & external pressure on the displacement and stresses was investigated. Some general conclusions were observed and summarized as follows:

1. Radial stress is zero at the outer surface in the case of internal pressure, zero at the inner surface in the case of external pressure, and non-zero on both sides in the case of both-sided

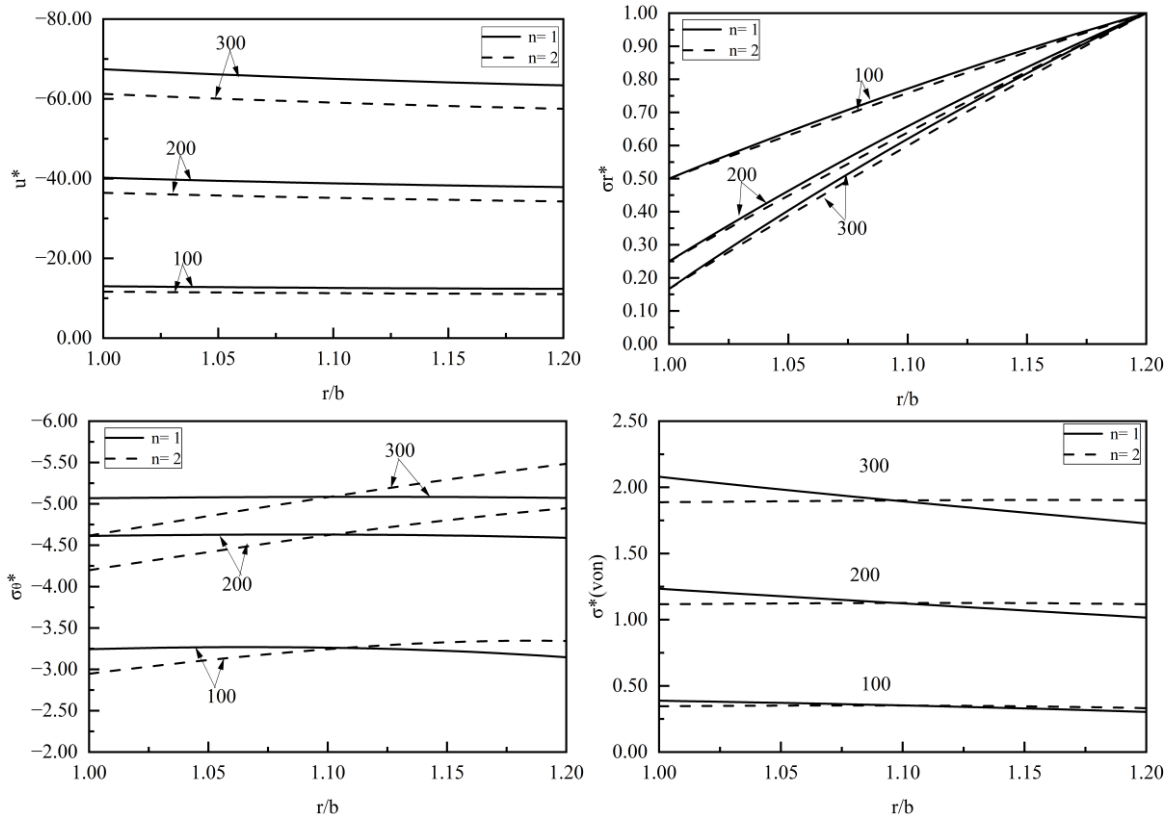

Fig. 12 Effect of various pressures (internal and external pressure) on displacement and stresses (radial, tangential and von Mises)

pressures. And in between the inner and outer radius, the radial stress variations remain tensile.

2. Due to the material parameter variations, the displacement and stresses have significant changes throughout the thickness in all cases considered as above, and omitting the different applications as requirements.

3. This study will help engineers design cylindrical vessels by analyzing the case study for different loading conditions considered in this paper.

References

Abbas, E.N., Abud Ali, Z.A.A., Njim, E.K., Flayyih, M.A. and Madan, R. (2025), "Analytical and numerical investigation of free vibration of nanoparticle-reinforced composite cylindrical shells", *Diagnostyka*, 1-12. https://doi.org/10.29354/diag/201249

Adiga, K., Herbert, M.A., Rao, S.S. and Shettigar, A. (2022), "Applications of reinforcement particles in the fabrication of Aluminium Metal Matrix Composites by Friction Stir Processing - A Review", *Manuf. Rev.*, **9**, 26. https://doi.org/10.1051/mfreview/2022025

Al-Furjan, M.S.H., Bolandi, S.Y., Habibi, M., Ebrahimi, F., Chen, G. and Safarpour, H. (2022), "Enhancing vibration performance of a spinning smart nanocomposite reinforced microstructure conveying fluid flow", *Eng. Comput.*, **38**(S5), 4097-4112.

https://doi.org/10.1007/s00366-020-01255-w

Alhous, Z.F.A., Jweeg, M.J., Njim, E.K., Mouthanna, A., Flayyih, M.A., Madan, R., Khobragade, P. and Rai, P.K. (2025), "Nonlinear frequency and dynamic response of PLA polymeric imperfect FG sandwich plates under hygrothermal conditions", *Coupled Syst. Mech.*, **14**(1), 1-19. https://doi.org/10.12989/csm.2025.14.1.001

Allam, M.N.M., Tantawy, R. and Zenkour, A.M. (2018), "Magneto-thermo-elastic response of exponentially graded piezoelectric hollow spheres", *Adv. Comput. Des.*, **3**(3), 303-318. https://doi.org/10.12989/acd.2018.3.3.303

Altabey, W.A. (2017), "A study on thermo-mechanical behavior of MCD through bulge test analysis", *Adv. Comput. Des.*, **2**(2), 107-119. https://doi.org/10.12989/acd.2017.2.2.107

Amirjan, M. and Bozorg, M. (2019), "Fabrication and properties of Cu-Al2O3 functionally graded nanocomposites prepared by spark plasma sintering: The effect of copper particle size and reinforcement content", *Mater. Res. Exp.*, **6**(10). https://doi.org/10.1088/2053-1591/ab34c5

Ansari, M., Jabari, E. and Toyserkani, E. (2021), "Opportunities and challenges in additive manufacturing of functionally graded metallic materials via powder-fed laser directed energy deposition: A review", *J. Mater. Proc. Technol.*, **294**, 117117. https://doi.org/10.1016/j.jmatprotec.2021.117117

Avcar, M. (2019), "Free vibration of imperfect sigmoid and power law functionally graded beams", *Steel Compos. Struct.*, **30**(6), 603-615. https://doi.org/10.12989/scs.2019.30.6.603

Bayat, M., Sahari, B.B., Saleem, M., Ali, A. and Wong, S.V. (2009), "Bending analysis of a functionally graded rotating disk based on the first order shear deformation theory", *Appl. Math. Modell.*, **33**(11), 4215-4230. https://doi.org/10.1016/j.apm.2009.03.001

Cinefra, M., Carrera, E., Brischetto ,S. and and Belouettar, S. (2010), "Thermo-mechanical analysis of functionally graded shells", *J. Therm. Stress.*, **33**(10), 942-963. https://doi.org/10.1080/01495739.2010.482379

Daneshmand, S., Vini, M.H., Sajadi, S.M., Mouthanna, A., Jasim, D.J., Hammoodi, K.A., Hekmatifar, M. and Nasajpour-Esfahani, N. (2023), "Numerical and experimental investigations of mechanical, tribological, and electrical properties of laminated Bi-metal Al/SiC/Ni composites", *Mater. Today Commun.*, **37**, 107355. https://doi.org/10.1016/j.mtcomm.2023.107355

Das, P., Benslimane, A., Islam, M.A., Mondal, D. and Nazim, M.S. (2024), "A thermo-mechanically loaded rotating FGM cylindrical pressure vessels under parabolic changing properties: An analytical and numerical analysis", *Heliyon*, **10**(4).

Eraslan, A.N. and Orcan, Y. (2002), "Elastic-plastic deformation of a rotating solid disk of exponentially varying thickness", *Mech. Mater.*, **34**(7), 423-432. https://doi.org/10.1016/S0167-6636(02)00117-5

Fallahi Arezodar, A. and Nikbakht, A. (2019), "Micromechanical modeling and investigating the effect of particle size and the interface of phases on the mechanical behavior of dual-phase steels", *J. Mater. Eng. Perform.*, **28**(1), 53-62. https://doi.org/10.1007/s11665-018-3768-x

Feng, S.Z. and Li, A.M. (2017), "Analysis of thermal and mechanical response in functionally graded cylinder using cell-based smoothed radial point interpolation method", *Aerosp. Sci. Technol.*, **65**, 46-53. https://doi.org/10.1016/j.ast.2017.02.00

Garg, A., Belarbi, M.O., Chalak, H.D. and Chakrabarti, A. (2021), "A review of the analysis of sandwich FGM structures", *Compos. Struct.*, **258**, 113427. https://doi.org/10.1016/j.compstruct.2020.113427

Habib, E.S., El-Hadek, M.A. and El-Megharbel, A. (2018), "Stress analysis for cylinder made of FGM and subjected to thermo-mechanical loadings", *Metals*, **9**(1), 4. https://doi.org/10.3390/met9010004

Hadji, L., Avcar, M. and Civalek, Ö. (2021), "An analytical solution for the free vibration of FG nanoplates", *J. Brazil. Soc. Mech. Sci. Eng.*, **43**(9), 418. https://doi.org/10.1007/s40430-021-03134-x

Hadji, L., Madan, R. and Bernard, F. (2024a), "Thermal buckling in multi-directional porous plates: The effects of material grading and aspect ratio", *Proceedings of the Institution of Mechanical Engineers, Part G: Journal of Aerospace Engineering*, **238**(4), 412-426. https://doi.org/10.1177/09544100241232132

Hadji, L., Plevris, V. and Madan, R. (2023), "A Static and Free Vibration Analysis of Porous Functionally Graded Beams", *Proceedings of the International Conference on Civil Infrastructure and Construction (CIC 2023)*, 433-441. https://doi.org/10.29117/cic.2023.0059

Hadji, L., Plevris, V., Madan, R. and Ait Atmane, H. (2024b), "Multi-directional functionally graded sandwich plates: buckling and free vibration analysis with refined plate models under various boundary conditions", *Computation*, **12**(4), 65. https://doi.org/10.3390/computation12040065

Hangai, Y., Ishihara, A., Utsunomiya, T., Kuwazuru, O. and Yoshikawa, N. (2016), "Fabrication of two layers porous aluminum varying porosity by friction powder sintering process and its compression properties", *Nippon Kinzoku Gakkaishi, J. Japan Inst. Metals*, **80**(6), 390-393. https://doi.org/10.2320/jinstmet.J2016017

Jabbari, M., Bahtui, A. and Eslami, M.R. (2009), "Axisymmetric mechanical and thermal stresses in thick short length FGM cylinders", *Int. J. Press. Vessels Pip.*, **86**(5), 296-306. https://doi.org/10.1016/j.ijpvp.2008.12.002

Jabbari, M., Sohrabpour, S. and Eslami, M.R. (2002), "Mechanical and thermal stresses in a functionally graded hollow cylinder due to radially symmetric loads", *Int. J. Press. Vessels Pip.*, **79**(7), 493-497. https://doi.org/10.1016/S0308-0161(02)00043-1

Kadum Njim, E., AlMaamori, M.H., Madan, R., Bakhy, S.H., AlWaily, M., Khobragade, P. and Hadji, L. (2024), "Numerical and analytical investigation of free vibration behavior of porous functionally graded sandwich plates", *Mech. Adv. Compos. Struct.*, **12**(3), 555-568. https://doi.org/10.22075/macs.2024.34962.1710

Lal, A., Jagtap, K.R. and Singh, B.N. (2017), "Thermo-mechanically induced finite element based nonlinear static response of elastically supported functionally graded plate with random system properties", *Adv. Comput. Des.*, **2**(3), 165-194. https://doi.org/10.12989/acd.2017.2.3.165

Lu, Y. and Chen, X. (2020), "Nonlinear parametric dynamics of bidirectional functionally graded beams", *Shock Vib.*, 1-13. https://doi.org/10.1155/2020/8840833

Madan, R. and Bhowmick, S. (2020), "A review on application of FGM fabricated using solid-state processes", *Adv Mater. Proc. Technol.*, **6**(3), 608-619. https://doi.org/10.1080/2374068X.2020.1731153

Madan, R. and Bhowmick, S. (2021), "Modeling of functionally graded materials to estimate effective thermo-mechanical properties", *World J. Eng.*, **19**(3), 91-301. https://doi.org/10.1108/WJE-09-2020-0445

Madan, R. and Bhowmick, S. (2022), "Fabrication, microstructural characterization and finite element analysis of functionally graded Al-Al2O3 disk using powder metallurgy technique", *Mater. Today Commun*, **32**, 103878. https://doi.org/10.1016/j.mtcomm.2022.103878

Madan, R., Bhowmick, S., Hadji, L. and Alnujaie, A. (2023), "Limit angular speed analysis of porous functionally graded rotating disk under thermo-mechanical loading", *Multidiscipl. Model. Mater. Struct.,* **19**(2), 311-323. https://doi.org/10.1108/MMMS-09-2022-0197

Muthanna, A., Ali. M., Hasan M.H., Najim. B.K., Njim, E.K., Madan R. and Mohammed H. Al-Maamori. (2025), "Vibration investigation of an imperfect FGM cylindrical shell reinforced by various types of stiffeners with temperature dependent properties resting on an elastic foundation", *Coupled Syst. Mech.*, **14**(2), 105-127. https://doi.org/10.12989/csm.2025.14.2.105

Nejad, M.Z., Jabbari, M. and Ghannad, M. (2015), "Elastic analysis of axially functionally graded rotating thick cylinder with variable thickness under non-uniform arbitrarily pressure loading", *Int. J. Eng. Sci.*, **89**, 86-99. https://doi.org/10.1016/j.ijengsci.2014.12.004

Njim, E.K., Bakhy, S.H. and Al-Waily, M. (2021), "Analytical and numerical investigation of free vibration behavior for sandwich plate with functionally graded porous metal core", *Pertanika J. Sci. Technol.*, **29**, 3.

Njim, E.K., Hasan, H.R., Jweeg, M.J., Al-Waily, M., Hameed, A.A., Youssef, A.M. and Elsayed, F.M. (2024), "Mechanical properties of sandwiched construction with composite and hybrid core structure", *Adv. Polym. Technol*, 1, 3803199. https://doi.org/10.1155/2024/3803199

Raad, H., Najim, E., Jweeg, M., AlWaily, M., Hadji, L. and Madan, R. (2024), "Vibration analysis of sandwich plates with hybrid composite cores combining porous polymer and foam structures", *J. Comput. Appl. Mech.*, **55**(3). https://doi.org/10.22059/jcamech.2024.377658.1121

Rahimi, G.H., Arefi, M. and Khoshgoftar, M.J. (2011), "Application and analysis of functionally graded piezoelectrical rotating cylinder as mechanical sensor subjected to pressure and thermal loads", *Appl. Math. Mech.*, **32**(8), 997-1008. https://doi.org/10.1007/s10483-011-1475-6

Reddy, J.N. and Chin, C.D. (1998), "Thermomechanical analysis of functionally graded cylinders and

plates", *J. Therm. Stress.*, **21**(6), 593-626. https://doi.org/10.1080/01495739808956165
Singh, A. and Kumari, P. (2020), "Analytical free vibration solution for angle-ply piezolaminated plate under cylindrical bending: A piezo-elasticity approach", *Adv. Comput. Des.*, **5**(1), 55-89. https://doi.org/10.12989/acd.2020.5.1.055
Singh, S.K., Sondhi, L., Sahu, R.K., Madan, R. and Yadav, S. (2024), "Investigating thermo-mechanical stresses in functionally graded disks using Navier's method for different loading conditions", *Struct. Eng. Mech.*, **91**(6), 627-642. https://doi.org/10.12989/sem.2024.91.6.627
Sondhi, L., Sahu, R.K., Kumar, R., Yadav, S., Bhowmick, S. and Madan, R. (2023), "Functionally graded polar orthotropic rotating disks: Investigating thermo-elastic behavior under different boundary conditions", *Int. J. Interact. Des. Manuf.*, **18**, 159-166. https://doi.org/10.1007/s12008-023-01447-w.
Sondhi, L., Thawait, A.K., Yadav, S., Bhowmick, S. and Madan, R. (2024), "Investigating stress and deformation behavior of functionally graded cylindrical shells under external pressure", *Proceedings of the International and National Conference on Machines and Mechanism,* Springer Nature Singapore, Singapore, pp. 371-384.
Suresh, S. and Mortensen, A. (1997), "Functionally graded metals and metal-ceramic composites: Part 2 Thermomechanical behaviour", *Int. Mater. Rev.,* **42**(3), 85-116. https://doi.org/10.1179/imr.1997.42.3.85
Tarn, J.Q. (2001), "Exact solutions for functionally graded anisotropic cylinders subjected to thermal and mechanical loads", *Int. J. Solids Struct.*, **38**(46), 8189-8206. https://doi.org/10.1016/S0020-7683(01)00182-2
Tutuncu, N. and Temel, B. (2009), "A novel approach to stress analysis of pressurized FGM cylinders, disks and spheres", *Compos. Struct.*, **91**(3), 385-390. https://doi.org/10.1016/j.compstruct.2009.06.009
Vasil'ev, V.V. and Fedorov, L.V. (2022), "Stress functions in elasticity theory", *Mech. Solids*, **57**(4), 770-778.
Vaziri, S.A., Ghannad, M. and Bég, O.A. (2019), "Exact thermoelastic analysis of a thick cylindrical functionally graded material shell under unsteady heating using first order shear deformation theory", *Heat Transf. Asian Res.*, **8**(5), 1737-1760. https://doi.org/10.1002/htj.21455
Viet, N.V., Zaki, W. and Wang, Q. (2020), "Free vibration characteristics of sectioned unidirectional/ bidirectional functionally graded material cantilever beams based on finite element analysis", *Appl. Math. Mech.*, **41**(12), 1787-1804. https://doi.org/10.1007/s10483-020-2664-8
Wang, Z.W., Zhang, Q., Xia, L.Z., Wu, J.T. and Liu, P.Q. (2015), "Stress analysis and parameter optimization of an fgm pressure vessel subjected to thermo-mechanical loadings", *Procedia Eng.*, 374-389. https://doi.org/10.1016/j.proeng.2015.12.230
Zenkour, A.M. and Abouelregal, A.E. (2018), "Decaying temperature and dynamic response of a thermoelastic nanobeam to a moving load", *Adv. Comput. Des.,* **3**(1), 1-16. https://doi.org/10.12989/acd.2018.3.1.001

CC

Nomenclature

a	Inner radius (m)	q_{rr}	Heat generation function (kj/m^3)
b	Outer radius (m)	E_a	Young's modulus at 'a' (MPa)
r	Radial direction (m)	α_a	CTE at 'a' ($per\ ^0C$)
u	Displacement component (m)	k_a	TCC at 'a' (W/mk)

ε_{rr}	Radial strain	$\rho_{a,}$	Density at 'a' (kg/m^3)
ε_{tt}	Tangential strain	q_a	Heat generation at 'a' (kj/m^3)
σ_{rr}	Radial stress (MPa)	$m_1 = m_2 = m_3 = m_4 = m_5$	Material grading parameter
σ_{tt}	Tangential stress (MPa)	T_{rr}	Temperature function (^0C)
ω	Rotation (rad/s)	T_a	Temperature at 'a' (^0C)
g	Gravity (m/s^2)	T_b	Temperature at 'b' (^0C)
Y_{rr}	Young's modulus function (MPa)	$Q_3,\ Q_4,\ P_3,\ P_4$	Thermal constants
α_{rr}	CTE function ($per\ ^0C$)	$Q_1,\ Q_2,\ P_1,\ P_2$	Displacement constants
k_{rr}	Thermal conduction coefficient (TCC) function (W/mk)	P_a	Pressure at inner radius (MPa)
ρ_{rr}	Density function (kg/m^3)	P_b	Pressure at outer radius (MPa)